

# Effect of pressure on nucleation and growth in the $\text{Zr}_{46.75}\text{Ti}_{8.25}\text{Cu}_{7.5}\text{Ni}_{10}\text{Be}_{27.5}$ bulk glass-forming alloy investigated using *in situ* x-ray diffraction

W. H. Wang,<sup>1,2,\*</sup> T. Okada,<sup>2</sup> P. Wen,<sup>1</sup> X.-L. Wang,<sup>3</sup> M. X. Pan,<sup>1</sup> D. Q. Zhao,<sup>1</sup> and W. Utsumi<sup>2</sup>

<sup>1</sup>*Institute of Physics, Chinese Academy of Sciences, Beijing 100080, China*

<sup>2</sup>*Japan Atomic Energy Research Institute, SPring-8, Hyogo 679-5198, Japan*

<sup>3</sup>*Spallation Neutron Source and Metals and Ceramics Division, Oak Ridge National Laboratory, Oak Ridge, Tennessee 37830, USA*

(Received 10 February 2003; revised manuscript received 16 July 2003; published 11 November 2003)

The effects of pressure up to 10 GPa on nucleation and growth in a typical  $\text{Zr}_{46.75}\text{Ti}_{8.25}\text{Cu}_{7.5}\text{Ni}_{10}\text{Be}_{27.5}$  (vit4) bulk glass-forming alloy during heating, isothermal annealing, and cooling processes were investigated using *in situ* x-ray diffraction with a synchrotron radiation. It is found that pressure has diverse effects on the nucleation and growth depending on different heat treatments. The constant heating under high pressure can affect the stability of the supercooled liquid state and increase the crystallization temperature. Isothermal high pressure annealing leads to nanocrystallization, which is attributed to the copious nucleation and slow growth velocity. Pressure can enhance the glass forming ability of the alloy by effectively suppressing the crystallization during cooling; bulk glass can be obtained by cooling the melt alloy under high pressure at low cooling rate. The various effects of high pressure on the nucleation and growth and the crystalline phases formed are discussed from the points of view of nucleation kinetics and thermodynamics.

DOI: 10.1103/PhysRevB.68.184105

PACS number(s): 61.43.Fs, 62.50.+p, 64.70.Dv, 81.20.-n

## I. INTRODUCTION

In-depth investigations of crystallization in metallic glasses are important for understanding the nucleation and growth in a metallic supercooled liquid, for evaluating the glass forming ability (GFA). Recently developed bulk glass forming alloys with a wide supercooled liquid region and high thermal stability against crystallization offer a large experimentally accessible time and temperature window to investigate the nucleation and growth in metallic liquid.<sup>1,2</sup> During the last decade crystallization at ambient extensively studied in a wide variety of bulk metallic glasses (BMGs).<sup>1,3-5</sup> The crystallization has been found to be sensitive to the external influences such as preannealing, kinetic conditions, and additions.<sup>3-10</sup> High pressure (HP), which is becoming an important processing variable just like that of temperature or chemical composition, has been found to be a powerful tool for affecting and controlling the nucleation and growth in the metallic glasses.<sup>7-14</sup>

Crystallization in BMGs is very complex due to the possible phase separation before the crystallization and complicated diffusion fluxes in the supercooled liquid state. The effect of pressure on metallic glasses is also complex. HP has been found to promote or suppress crystallization in different glasses.<sup>15-17</sup> For example, Shen *et al.*<sup>12</sup> found that appropriate pressure could lower or raise activation energy of the crystallization. For a BMG with a complicated multistage crystallization process, the effect of pressure on the crystallization temperature,  $T_x$  depends on the applied pressure range and time. One thus cannot simply extrapolate or compare the effect of pressure on  $T_x$  in different pressure ranges. Meanwhile, the different techniques used to study the crystallization may also result in different observations. X-ray diffraction (XRD) has a limit to detect the precipitation of nanocrystalline particles in the amorphous matrix induced by primary crystallization. The high-resolution transmission electron microscope and differential scanning calorimeter

(DSC) are more sensitive ways to detect the primary nanocrystallization. The crystallization also depends strongly on the treatment process, heating or cooling rate, and annealing time.<sup>18-20</sup> For example  $T_x$  of  $\text{Zr}_{41}\text{Ti}_{14}\text{Cu}_{14.5}\text{Ni}_{10}\text{Be}_{22.5}$  BMG (vit1) obtained from the DSC, with heating rates of 5 and 80 K/min, are 683 and 742 K, respectively.<sup>19</sup> Schroers *et al.*<sup>21</sup> reported that a heating rate of 200 k/s could even avoid any crystallization in vit1. It is found that a nanocrystallization occurs in vit1 when annealed at 623 K [much lower than  $T_x = 698$  K (Ref. 19)] for a long time at vacuum.<sup>20</sup> Different researchers sometime obtained alternative and even contradictory results due to their different pressure annealing conditions and detecting methods applied.<sup>22</sup> Therefore, it is necessary to systematically study the effects of pressure on the nucleation and growth in BMGs and to clarify the role of the pressure on the phase evolution during crystallization. On the other hand, the ability to form a glass by cooling from the melt is equivalent to suppressing crystallization. Applying HP during the solidification of a glass-forming alloy may improve the GFA, and provide a useful way to study the glass formation mechanism.

In this work, we chose the typical  $\text{Zr}_{46.75}\text{Ti}_{8.25}\text{Cu}_{7.5}\text{Ni}_{10}\text{Be}_{27.5}$  alloy (vit4) to study the effects of HP on the crystallization of glass forming alloys. The reasons for choosing vit4 lie in the facts that the supercooled liquid of vit4 is considered as one of the most stable metallic liquids known at ambient pressure.<sup>1</sup> In contrast to simple metallic liquids and most alloys, vit4 has a wide supercooled liquid region which provides an ideal alloy system for studying pressure effects on the nucleation and growth of the crystalline phase in the supercooled liquid without intervening phase separation. XRD with synchrotron radiation was used to monitor *in situ* the nucleation and growth of the alloy during isothermal annealing, cooling and heating process in pressure range of 0–10 GPa. The effects of HP on crystallization are discussed from the point of view of nucleation theory.

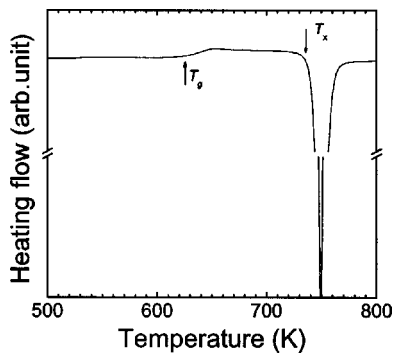


FIG. 1. DSC trace of the  $Zr_{46.75}Ti_{8.25}Cu_{7.5}Ni_{10}Be_{27.5}$  BMG at a heating rate of 0.33 K/s.

## II. EXPERIMENTAL PROCEDURES

$Zr_{46.75}Ti_{8.25}Cu_{7.5}Ni_{10}Be_{27.5}$  bulk metallic glass was prepared by casting the molten alloy in a water-cooling Cu mold to obtain a rod with a diameter of 8 mm. The amorphous nature as well as the homogeneity of the rod was ascertained with XRD and the transmission electron microscope.<sup>3</sup> The crystallization of the alloy was investigated by an *in situ* XRD technique at Spring-8, a third-generation synchrotron radiation facility in Japan. High-pressure and high-temperature conditions were generated using a cubic-type multianvil press (SMAP 180) installed on BL14B1.<sup>23</sup> The sample assembly was similar to that used in Ref. 24. A NiCr-NiAl thermocouple was brought into the pressurized zone and near the sample. NaCl powder was used as the pressure transmitting medium. The pressure was calibrated from the lattice constant of NaCl, and the accuracy was better than  $\pm 0.2$  GPa. For the cooling experiments, the sample was first pressurized to HP, and then heated to 1373 K and kept in the condition for about 5 min. After that, the heating electrical current was switched off and the sample was naturally cooled down under HP. An energy dispersive method was utilized using a white x ray with energies of 40–150 keV. The diffracted x ray was detected by a solid state Ge detector, at a diffraction angle  $2\theta = 5^\circ$ . The structure of the recovered samples was also checked by XRD using a Rigaku, Rapid-XRD diffractometer with  $Cu K_\alpha$  radiation. DSC measurements were carried out under a purified argon atmosphere in a Perkin Elmer DSC-7.

## III. RESULTS AND DISCUSSION

Figure 1 shows DSC traces of the  $Zr_{46.75}Ti_{8.25}Cu_{7.5}Ni_{10}Be_{27.5}$  BMG at a heating rate of 0.33 K/s. The glass transition temperature  $T_g$ , and the onset temperature of crystallization  $T_x$  are 620 and 735 K, respectively. A remarkable feature is a significantly large supercooled liquid region ( $\Delta T = T_x - T_g = 115$  K) indicating high stability of the supercooled liquid state of vit4.<sup>1</sup> Unlike other BMGs, no decomposition has been observed in vit4 at ambient pressure.<sup>20,25–28</sup> So, vit4 is an ideal alloy to study the crystallization of the metallic liquid. Figure 2 presents XRD patterns of vit4 annealed at various temperatures for about 0.1 h at ambient pressure. The BMG does not show XRD

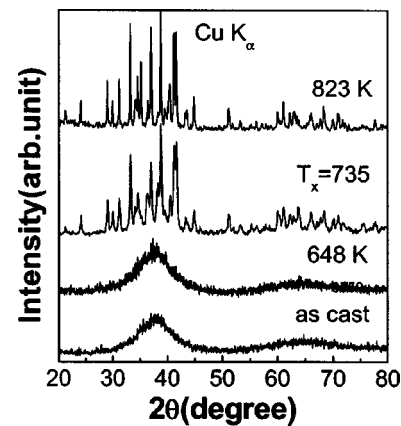


FIG. 2. XRD patterns of vit4 at various temperatures under ambient pressure.

detectable crystallization when annealed in the supercooled liquid region. However, the BMG almost completely crystallized when annealed at  $T_x$ , the XRD patterns of the annealed specimens at 735 and 823 K are almost identical. The result indicates that vit4 behavior is a collective crystallization occurring in a very narrow increasing temperature range similar to that of other BMGs.<sup>5,8,28–30</sup> When the vit alloys including vit4 were isoannealed in the low temperature region in supercooled liquid state (near  $T_g$ ), a primary metastable quasicrystalline phase will form, and the metastable phase transforms into stable crystalline phases at high temperature.<sup>28,30</sup> The main final crystallized phases are  $ZrBe_2$ , laves-phase  $ZrTiNi$ ,  $Zr_2Cu$ , and other unidentified phases.<sup>28,30</sup>

### A. Effect of pressure on crystallization during heating

Figure 3 shows the synchrotron radiation XRD patterns of vit4 measured *in situ* at various temperatures under 10.1 GPa. Up to 743 K (higher than  $T_x$  at ambient pressure), the amorphous state is retained without clear indication of crystallization within the limit of XRD. The BMG starts to crystallize at about 743 K, and a 40-K increase only causes a partial crystallization, indicating that vit4 is not again a col-

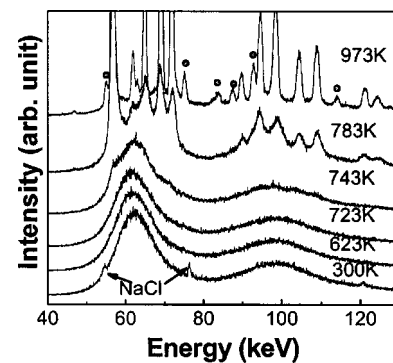


FIG. 3. *In situ* synchrotron XRD patterns of the  $Zr_{46.75}Ti_{8.25}Cu_{7.5}Ni_{10}Be_{27.5}$  BMG at elevating temperature under 10.1 GPa. After full crystallization (at 973 K) the final crystallization involves additional phases, and other intermetallic compounds as marked.

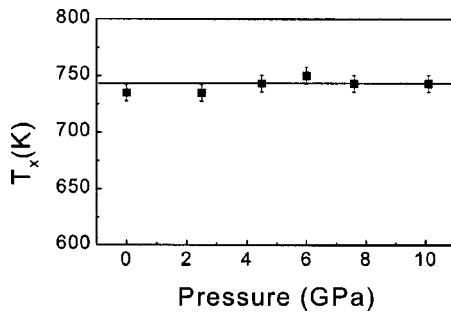


FIG. 4. Onset of the crystallization temperature of the vit4 under various pressures. When we determine  $T_x$  by *in situ* XRD, the temperature is increased in steps of 5 K, so the determined values of  $T_x$  has an error of  $\pm 5$  K.

lective crystallization under HP (vit4 is single-stage crystallization at ambient pressure as shown in Fig. 1). The primary precipitation phase is mainly a  $\text{MgZn}_2$  type of Laves phase  $\text{ZrTiNi}$ , and no metastable phases form during the HP heating process. The competition between the stable crystalline phases and intermediate metastable phases is controlled by thermodynamic and kinetic factors. The stable crystalline phases are thermodynamically favored because they have a lower free energy level compared to metastable phase. While the metastable phase is kinetically favored due to its lower nucleation barrier compared to crystalline phases which is similar to the solid state amorphization reaction.<sup>31</sup> Temperature and pressure are two different variables which affect the crystallization. Whereas temperature mainly affects the energy of supercooled liquid attempting to surmount activation barriers, pressure changes interatomic distances and subsequently the height of the barriers.<sup>11</sup> We infer that HP can reduce the activation barriers for a stable crystalline phase, and make them favorable in the crystallization competition. This is confirmed by our recent work that the HP can reduce the nucleation activation barriers from 5.0 eV at ambient pressure to 2.5 eV under 4.5 GPa for a Cu-based BMG.<sup>32</sup> HP thus changes the crystallization phase evolution. The fully crystallization is reached at 973 K during heating (the average heating rate is less than 0.167 K/s and lower than the heating rate used in Fig. 1). After complete crystallization, the final crystallization involves additional phases, and other intermetallic compounds, e.g.,  $\text{Zr}_2\text{Cu}$ ,  $\text{Be}_2\text{Zr}$ , etc. The identification of the crystallized phases is very difficult due to the multicomponent alloy, and some crystalline peaks in the diffraction pattern do not exactly match any previously known phases. However, from a comparison with crystallization results at ambient pressure, the final crystallized products under HP (in the range of 0–10 GPa) are similar to that at ambient pressure, but the phase evolution procedures are different. The XRD results indicate that  $T_x$  is increased to about 743 K under pressure of 10.1 GPa, and the crystallization process happen at a larger temperature and time ranges under HP, and is not collective behavior. This is marked different from the crystallization process at ambient condition shown in Fig. 2. We have studied the crystallization of vit4 under various pressures (from 2.5 to 10.1 GPa). As shown in Fig. 4, the values of  $T_x$  are always around 745 K and do not show significant changes with pressure in the pressure range stud-

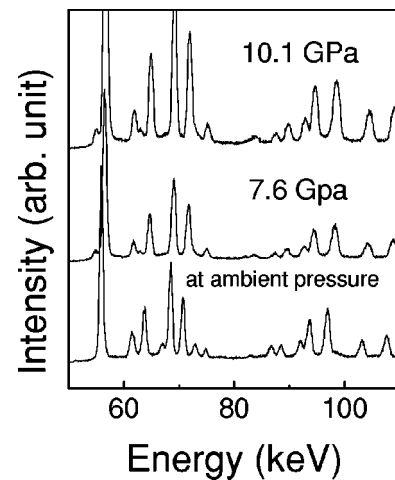


FIG. 5. A comparison of XRD patterns of vit4 crystallized under high pressure and at ambient pressure.

ied. This observation agrees with the results in Ref. 22, in which the crystallization temperature was found to increase linearly with pressure having a large slope of 1.7 K/GPa. The above results indicate that pressure plays a role in the suppression of the growth of the nuclei in vit4.  $T_x$  is increased by about 10 K in the pressure range of 2–10 GPa, but does not show a collective behavior. Figure 5 show a comparison of XRD patterns of the crystallization products of vit4 fully crystallized under various pressures at 973 K (at 10.1 GPa, and 7.6 GPa, and at ambient pressure, respectively). Under HP, the final crystallized products are similar to that at ambient pressure.

#### B. Effect of pressure on crystallization during isothermal annealing

Figure 6 gives *in situ* XRD patterns of vit4 annealed at 713 K ( $< T_x$ ) under 7.6 GPa upon annealing time. The sample exhibits no significant difference compared to that of the as-prepared BMG in the first 30 min. At a longer anneal-

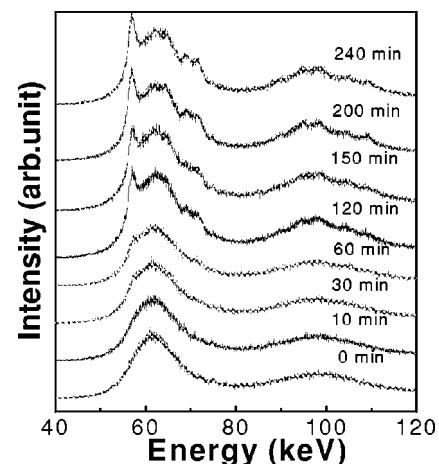


FIG. 6. *In situ* synchrotron XRD patterns of the  $\text{Zr}_{46.75}\text{Ti}_{8.25}\text{Cu}_{7.5}\text{Ni}_{10}\text{Be}_{27.5}$  BMG isothermal annealed at 713 K under 7.6 GPa.

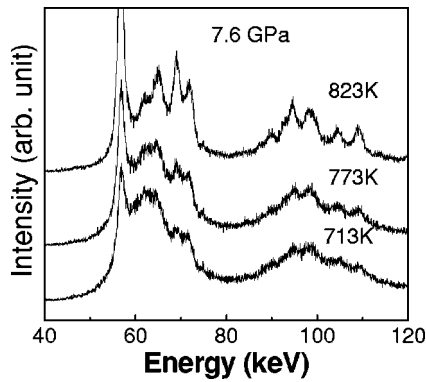


FIG. 7. *In situ* XRD patterns of the  $Zr_{46.75}Ti_{8.25}Cu_{7.5}Ni_{10}Be_{27.5}$  BMG (after isothermal annealing at 713 K under 7.6 GPa for 4.0 h) at high temperature under 7.6 GPa.

ing time, however, the XRD patterns show some broadened peaks that start to emerge on the amorphous diffuse peak, indicating the formation of nanosized crystalline particles and the occurrence of the crystallization. The crystalline reflections become significantly intensified and more peaks appear after more than 60 min annealing. The process continues with prolonged annealing and the crystallization reached saturation after 240 min. Figure 7 presents *in situ* XRD patterns during heating after annealing at 713 K for 240 min under 7.6 GPa. Up to 773 K, there are no significant changes in the peak number and intensity of the XRD pattern, indicating that the crystallization is not sensitive to the 60-K temperature increase. Meanwhile, the phase identification shows that the isothermal annealing induced crystallization involves no additional phases in the whole crystallization process, which can be explained as grain growth as the diffraction patterns are quite similar, as shown in Figs. 6 and 7. Based on the above results, we infer that the prolonged annealing causes almost full nanocrystallization in BMG. The subsequent elevating temperature cannot result in a marked change of the crystallization because the nanocrystallization during the isothermal annealing has already consumed almost all the amorphous phase in the alloy.

### C. Effect of pressure on crystallization during cooling process

Figure 8 shows the *in situ* XRD patterns of vit4 alloy during melting and cooling process at 7.6 GPa. The BMG fully crystallizes at 973 K, and is fully melted at 1373 K. After quenching to 300 K under 7.6 GPa, the samples with the applied pressure show a broad scattering peak, indicating the formation of a full amorphous phase. The  $ZrTiCuNiBe$  alloy cooled at a similar cooling rate without applied pressure consists mostly of crystalline phases, because the sample was covered with thick pyrophyllite and  $ZrO_2$  with low thermal conductivity, the solidifying heat release condition for the molten was very poor compared with that of the die cast in water cooling Cu mold, the cooling rate under HP (about 20 K/s) is much less than the critical cooling rate (about 100 K/s) for the fully glassy formation of vit4.<sup>1,33,34</sup> The XRD traces for the alloy cooled under different pressures are given in Fig. 9. The samples with a higher applied pressure (>6 GPa) show a broad scattering peak indicating

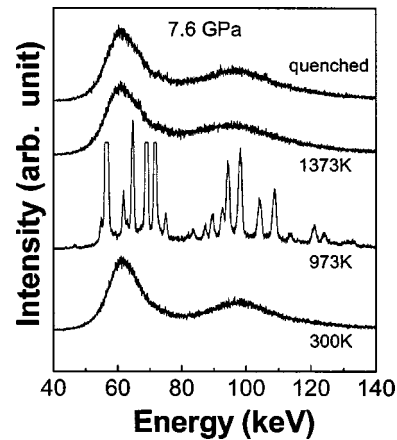


FIG. 8. Synchrotron XRD patterns of the  $Zr_{46.75}Ti_{8.25}Cu_{7.5}Ni_{10}Be_{27.5}$  alloy cooled under 7.6 GPa at various temperatures.

the full amorphous phase. However, when quenching at lower pressure (4.5 GPa), there are few weak sharp crystalline peaks superimposed on the broad peak, meaning that full amorphization cannot be reached. When cooling at much lower pressure (2.5 GPa), more fraction of crystalline phases form. The sample cooled with a similar cooling rate ( $\sim 20$  K/s) at ambient pressure consists of mostly crystalline phases.<sup>34</sup> The XRD result indicates that the GFA of vit4 is enhanced under HP. The increased GFA of the alloy under HP confirms that the kinetic factor such as the atomic mobility and viscosity of the melt is the key factor in the formation of BMGs.<sup>1</sup> Pressure also causes the melting temperature of the alloys to increase by about 110 K and leads to a larger undercooling of the liquid alloy, and the high undercooling leads to higher activation energy and slow growth rate for nucleation during the solidification.<sup>35,36</sup> This is a thermodynamic factor for the enhanced GFA. Figure 10 exhibits the different states of vit4 alloy at 7.6 GPa. The glassy state of the alloy obtained by high pressure quenching shows no significant difference compared to its supercooled liquid, the melt, and the glass state obtained by die cast. It is worth noting that HP is more effective for a suppression the crys-

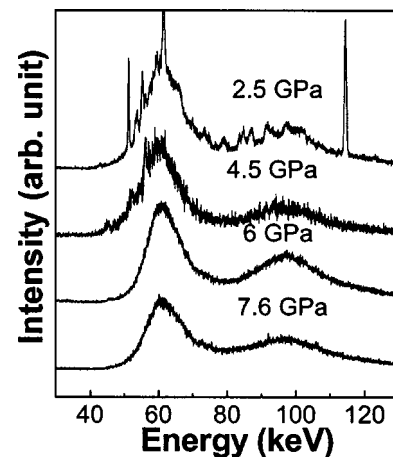


FIG. 9. The  $Zr_{46.75}Ti_{8.25}Cu_{7.5}Ni_{10}Be_{27.5}$  alloy cooled at roughly the same cooling rate under various pressures.

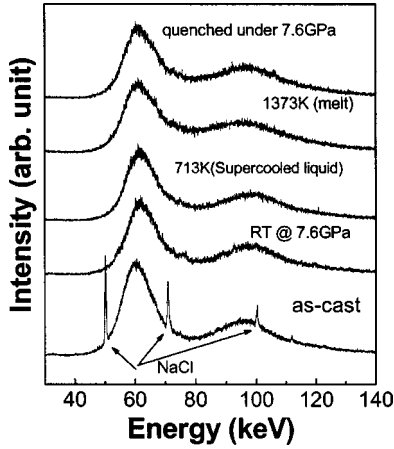


FIG. 10. The  $Zr_{46.75}Ti_{8.25}Cu_{7.5}Ni_{10}Be_{27.5}$  alloy at different states under 7.6 GPa.

tallization of the melt in the cooling process; a pressure of more than 6 GPa can completely suppress the growth of the nuclei, and transform the melt into a full glass. While  $T_x$  can only be slightly increased at 10 GPa upon heating, vit4 shows an asymmetry in crystallization behavior during heating and cooling under HP.

To simplify the analysis, we assume that there is only homogeneous nucleation during the crystallization in the alloy. Then, the effect of pressure on the nucleation activation energy,  $\Delta G^*$ , can be expressed as<sup>37</sup>

$$\left(\frac{\partial(\Delta G^*)}{\partial P}\right) = -\frac{32\pi\sigma^3}{3} \frac{\Delta V}{(\Delta G)^3},$$

where  $\sigma$  is interfacial energy, which is not sensitive to pressure, and  $\Delta G = G_a - G_c$  is the free energy difference between the amorphous state  $G_a$  and crystalline state  $G_c$ ,  $\Delta V = V_a - V_c$  is the difference of molar volumes between the amorphous phase  $V_a$  and the crystalline phase  $V_c$ . For vit4,  $\partial(\Delta G^*)/\partial P < 0$ , since the volume per molar is decreased after crystallization from liquid or amorphous phase,<sup>38</sup> i.e.,  $\Delta V = V_a - V_c > 0$ . This means that pressure will lead to a decrease of the nucleation activation energy and the critical nuclei size, and promote the nucleation in the supercooled liquid. Other experimental and numerical modeling studies also demonstrate that HP promotes short-range atomic ordering in the metallic glasses.<sup>11-12</sup> The effect of pressure on growth is described by

$$\left(\frac{\partial(\ln D)}{\partial P}\right)_T = -\frac{\Delta V^*}{k_B T}.$$

Here  $D$  is the diffusivity,  $k_B$  is the Boltzmann constant, and  $\Delta V^*$  is the activation volume. For vit4,  $\Delta V^* = 13.0 \text{ \AA}^3 > 0$ ,<sup>39</sup> then,  $\partial(\ln D)/\partial P < 0$ . This means that  $D$  decreases with increasing pressure. At ambient pressure  $p\Delta V^*$  of the BMG is in the order of  $10^{-6}$  eV, and the pressure effect is negligible compared to the temperature effect, (the temperature effect is  $k_B T$ , which is about 0.1 eV/atom when the temperature is increased to 800 K from room temperature) and activation energy of diffusion in BMGs ( $\sim 1.0$  eV).<sup>40</sup> However, the effect of pressure for the diffusion cannot be ignored when

pressure reaches the GPa level; the increasing diffusion activation energy upon pressure is about 0.05 eV/GPa in vit4.

Based on the above analysis, owing to the intrinsic extremely low atomic mobility under pressure for diffusion, the atomic redistribution on a large-range scale is more difficult, and the subsequent growth of the nucleation sites is inhibited, this will result in the increased  $T_x$  of the BMG under HP detected by XRD during the constant heating process. However, HP further accelerates the nucleation by changing the atomic mobility in the short range. Therefore, the critical nucleus size decreases and some undercritical clusters become overcritical nuclei. Therefore, when the BMG is isothermally annealed below  $T_x$  under HP, nanocrystallization occurs. HP, on the one hand, leads to more copious nucleation through decreasing the nucleation energy barrier.<sup>26</sup> On the other hand, HP is an obstacle to the long-range atomic diffusion during the growth process due to the intrinsic extremely low atomic mobility under pressure. The contrary effects of HP on nucleation and growth cause nanocrystallization.

Vit4 shows an asymmetry in crystallization behavior during heating and cooling under HP. This results from the different maximum temperatures of the nucleation and growth rates. The maximum of the growth rate is at a much higher temperature than that of the nucleation rate in the alloy.<sup>21</sup> Therefore, when heating the BMG under HP, the alloy will first reach the temperature where the nucleation rate has a maximum, and a larger number of nuclei will be formed, promoted by HP. During further heating, the formed nuclei are exposed to the maximum growth rate, resulting in a high crystallization rate even HP suppresses the growth. In contrast, upon cooling the alloy from melt, at the temperature where the melt has the maximum growth rate, the alloy has few nucleus sites and nucleation rate, and the maximum number of nuclei formed at the same temperature experience low growth rate during further cooling, and lead to low crystallization rate. This means the nuclei, formed during cooling and heating, are exposed to different growth rates under high pressure and lead to the asymmetry in crystallization.

#### IV. CONCLUSIONS

Pressure has significant effects on nucleation and growth of vit4 BMG; however, the glass shows markedly different crystallization behaviors depending on heating procedures. The constant heating under HP can slightly increase  $T_x$  in the BMG. An isothermal HP anneal leads to nanocrystallization, which can be attributed to the copious nucleation and slow growth velocity induced by HP annealing. The BMG shows an asymmetry in crystallization behavior during heating and cooling under HP, pressure can enhance the GFA of the alloy by effectively suppressing the growth of the crystalline phases during cooling, and more than a 6-GPa pressure can completely suppress the growth of the nuclei and obtain a full amorphous phase at a low cooling rate. Much higher pressure and a critical heating rate are needed to avoid the crystallization of the glassy alloy. The results indicate that the nuclei, formed during cooling and heating, are exposed to different growth rates under HP. Under HP, the final crystal-

lized products are similar to that at ambient pressure, but no intermediate metastable phases form in various annealing processes.

### ACKNOWLEDGMENTS

The authors are grateful for the financial support of the National Natural Science Foundation of China (Grant Nos.

59925101 and 50031010). W.H.W. is thankful for the financial support from Japanese Sciences Promotion Society. X.L.W. acknowledges support by the U.S. Department of Energy, Basic Energy Sciences, Division of Materials Science and Engineering, under Contract No. DE-AC05-00OR22725 with UT-Battelle, LLC. Dr. Y. Katayama, Dr. H. Kaneko, and Professor N. Hamaya are appreciated for valuable discussions.

\*Corresponding author. Email address: whw@aphy.iphy.ac.cn

- <sup>1</sup>W.L. Johnson, *MRS Bull.* **24**, 42 (1999).
- <sup>2</sup>A.L. Greer, *Science* **267**, 1947 (1995).
- <sup>3</sup>W.H. Wang, *Science des matériaux* **27**, 99 (1995).
- <sup>4</sup>A. Inoue, *Acta Mater.* **48**, 279 (2000).
- <sup>5</sup>J. Schroers, Y. Wu, R. Busch, and W.L. Johnson, *Acta Mater.* **49**, 2773 (2001).
- <sup>6</sup>W.H. Wang, Q. Wei, and H.Y. Bai, *Appl. Phys. Lett.* **71**, 58 (1997).
- <sup>7</sup>W.H. Wang, D.W. He, D.Q. Zhao, Y.S. Yao, and M. He, *Appl. Phys. Lett.* **75**, 2770 (1999).
- <sup>8</sup>W.H. Wang, Y.X. Zhuang, M.X. Pan, and Y.S. Yao, *J. Appl. Phys.* **88**, 3914 (2000); W.H. Wang, L.L. Li, and R.J. Wang, *Phys. Rev. B* **62**, 11292 (2001).
- <sup>9</sup>J. Saida, A. Inoue, M.W. Chen, and T. Sakurai, *Appl. Phys. Lett.* **75**, 3497 (1999).
- <sup>10</sup>D.Q. Zhao, M.X. Pan, and W.H. Wang, *Mater. Trans., JIM* **41**, 1427 (2000).
- <sup>11</sup>M. Yousuf and K.G. Rajan, *J. Mater. Sci. Lett.* **3**, 149 (1984).
- <sup>12</sup>Z.Y. Shen, G.Y. Chen, Y. Zhang, and X.J. Yin, *Phys. Rev. B* **39**, 2714 (1989).
- <sup>13</sup>W.K. Wang, H. Iwasaki, and K. Fukamichi, *J. Mater. Sci.* **15**, 2701 (1980).
- <sup>14</sup>J. Zhang, K.Q. Qiu, H.F. Zhang, and Z.Q. Hu, *J. Mater. Res.* **17**, 2935 (2002).
- <sup>15</sup>W.K. Wang, H. Iwasaki, and T. Masumoto, *J. Mater. Sci.* **8**, 3765 (1982).
- <sup>16</sup>W.K. Wang, *Acta Phys. Sinica* **33**, 908 (1982).
- <sup>17</sup>F. He and K. Lu, *Acta Mater.* **47**, 2449 (1999).
- <sup>18</sup>R. Busch, *JOM J. Minerals* **52**, 39 (2000).
- <sup>19</sup>W.H. Wang, Y.X. Zhuang, M.X. Pan, and Y.S. Yao, *J. Appl. Phys.* **88**, 3914 (2000).
- <sup>20</sup>S. Schneider, P. Thiyagarajan, and W.L. Johnson, *Appl. Phys. Lett.* **68**, 493 (1996).
- <sup>21</sup>J. Schroers, A. Masuhr, W.L. Johnson, and R. Busch, *Phys. Rev. B* **60**, 11855 (1999).
- <sup>22</sup>J.Z. Jiang, L. Gerward, and Y.S. Xu, *Appl. Phys. Lett.* **81**, 4347 (2000).
- <sup>23</sup>W. Utsumi, K. Funakoshi, S. Urakawa, M. Yamakata, K. Tsuji, H. Konishi, and O. Shimomura, *Rev. High Pressure Sci. Technol.* **7**, 1484 (1998).
- <sup>24</sup>V. Turkevich, T. Okada, W. Utsumi, and A. Garan, *Diamond Relat. Mater.* **11**, 1769 (2002).
- <sup>25</sup>W.H. Wang, Q. Wei, M.P. Macht, and H. Wollenberger, *Appl. Phys. Lett.* **71**, 1053 (1997).
- <sup>26</sup>M.X. Pan, and W.H. Wang, *Appl. Phys. Lett.* **78**, 601 (2001).
- <sup>27</sup>J.F. Loeffle and W.L. Johnson, *Scr. Mater.* **44**, 1251 (2001).
- <sup>28</sup>T.A. Waniuk, J. Schroers, and W.L. Johnson, *Appl. Phys. Lett.* **78**, 1213 (2001); *Phys. Rev. B* **67**, 184203 (2003).
- <sup>29</sup>J. Schroers and W.L. Johnson, *Appl. Phys. Lett.* **76**, 2343 (2000); *J. Appl. Phys.* **88**, 44 (2000).
- <sup>30</sup>W.H. Wang, E. Wu, R.J. Wang, S.J. Kennedy, and A.J. Studer, *Phys. Rev. B* **66**, 104205 (2002).
- <sup>31</sup>W.L. Johnson, *Prog. Mater. Sci.* **30**, 81 (1986).
- <sup>32</sup>Z.X. Wang, W.H. Wang, and W. Utsumi (unpublished).
- <sup>33</sup>W.H. Wang, Q. Wei, and S. Friedrich, *Phys. Rev. B* **57**, 8211 (1998).
- <sup>34</sup>W.H. Wang, R.J. Wang, M.X. Pan, and Y.S. Yao, *Appl. Phys. Lett.* **79**, 1106 (2001).
- <sup>35</sup>D. Turnbull, *Prog. Solid State Phys.* **3**, 225 (1956).
- <sup>36</sup>H.J. Fecht, *Mater. Trans., JIM* **36**, 777 (1995).
- <sup>37</sup>D. Turnbull and J.C. Fisher, *J. Chem. Phys.* **17**, 71 (1949).
- <sup>38</sup>W.H. Wang, H.Y. Bai, J.L. Luo, R.J. Wang, and D. Jin, *Phys. Rev. B* **62**, 25 (2000).
- <sup>39</sup>P. Wen and W.H. Wang (unpublished).
- <sup>40</sup>X.P. Tang, U. Geyer, R. Busch, W.L. Johnson, and Y. Wu, *Nature (London)* **402**, 160 (1999).